[DOI]10.12016/j.issn.2096-1456.2021.04.002

·基础研究·

新型钛表面微纳米共存梯度仿生结构对骨髓间充质细胞黏附、增殖及成骨分化的影响

王旻，姜楠，祝颂松
口腔疾病研究国家重点实验室 国家口腔疾病临床医学研究中心 四川大学华西口腔医院口腔医院颌面外科，四川 成都(610041)

【摘要】 目的 制备一种新型微纳米共存梯度仿生表面结构，并探究其对骨髓间充质细胞生物学活性的影响。**方法** 通过放电等离子烧结法和阳极氧化处理分别在纯钛表面(纯钛组)制备微米骨小梁样结构(微米骨小梁组)和TiO_2纳米管形貌(TiO_2纳米管组)；再通过阳极氧化法在微米骨小梁样结构上制备TiO_2纳米管结构，形成新型微纳米共存梯度仿生表面结构，命名为微纳米复合钛组。应用扫描电子显微镜(scanning electronmicroscopy，SEM)和原子力显微镜(atomic force microscopy，AFM)、接触角(contact angle，CA)测量对纯钛组、微米骨小梁组、TiO_2纳米管组和微纳米复合钛组进行表征观察。将大鼠骨髓间充质细胞(bone marrow mesenchymal cells，BMMCs)接种于4组材料上，SEM观察细胞黏附情况；MTT法检测细胞在材料表面增殖能力；碱性磷酸酶(alkaline phosphatase，ALP)活性检测细胞在材料表面分化能力；共聚焦显微镜(confocal laser scanning microscope，CLSM)下观察细胞黏附、免疫荧光检测相关蛋白肌动蛋白(F-actin)、黏着斑蛋白(vinculin)、骨钙素(osteocalcin，OCN)、骨桥蛋白(osteopontin，OPN)表达；qRT-PCR观察细胞成骨转录因子RUNX2、OCN、OPN、I型胶原(collagen I，COLI)表达情况。**结果** 微纳米复合钛组表面亲水性最好(CA为9°±2.1°)；MTT结果示5～9 d，微纳米复合钛组和TiO_2纳米管组的细胞增殖活性显著高于纯钛组和微米骨小梁组($P<0.001$)；ALP结果示14 d时，微纳米复合钛组表面ALP活性最高；CLSM结果示培养24 h后，微纳米复合钛组肌动蛋白(F-actin)染色最深；培养72 h后，微纳米复合钛组OCN、OPN表达强于微米骨小梁组和TiO_2纳米管组。qRT-PCR结果示TiO_2纳米管组和微纳米复合钛组表面细胞所有成骨转录因子RUNX2、OCN、OPN、COLI的基因表达水平强于纯钛组和微米骨小梁组，其中I型胶原COLI基因表达水平差异有统计学意义($P<0.001$)。**结论** 微纳米复合钛这种新型微纳米共存梯度仿生表面结构能有效促进骨髓间充质细胞黏附、增殖及成骨向分化。

【关键词】 微纳米结构；TiO_2纳米管；仿生；表面处理；种植体；骨髓间充质细胞；细胞黏附；细胞增殖；成骨分化；放电等离子烧结；阳极氧化处理
【中图分类号】 R78　**【文献标志码】** A　**【文章编号】** 2096-1456(2021)04-0226-08
开放科学(资源服务)标识码(OSID)
【引用著录格式】 王旻，姜楠，祝颂松. 新型钛表面微纳米共存梯度仿生结构对骨髓间充质细胞黏附、增殖及成骨分化的影响[J]. 口腔疾病防治, 2021, 29(4): 226-233. doi: 10.12016/j.issn.2096-1456.2021.04.002.

A novel biomimetic micro/nano hierarchical interface of titanium enhances adhesion, proliferation and osteogenic differentiation of bone marrow mesenchymal cells

WANG Min, JIANG Nan, ZHU Songsong. State Key Laboratory Oral Diseases, National Clinical Reasearch Center for oral Diseases, Department of oral and Maxillofacial Surgery, West China Hospital of Stomatology, Sichuan University, Chengdu 610041, China
Corresponding author: ZHU Songsong, Email: zss_1977@163.com, Tel: 86-28-85503530

【Abstract】 Objective To design a novel biomimetic micro/nano hierarchical interface on endosseous titanium im-

【收稿日期】2020-08-24；**【修回日期】**2020-10-19
【基金项目】国家自然科学基金(81901026)
【作者简介】王旻，医师，硕士研究生在读，Email：15882167039@163.com
【通信作者】祝颂松，教授，博士，Email：zss_1977@163.com，Tel：86-28-85503530

plants and investigate its effect on the biological activity of bone marrow mesenchymal cells. **Methods** Electrochemical anodization and spark plasma sintering were used to modify smooth titanium (untreated Ti group) with a microporous trabecular bone-like architecture (micro-Ti group) and TiO_2 nanotube architecture (nano-TiO_2 group). Additionally, electrochemical anodization was employed to prepare TiO_2 nanotubes on microporous trabecular bone-like architectures, which formed a novel biomimetic hierarchical interface (micro/nano-TiO_2 group). Four groups of titanium samples were characterized by field emission scanning electron microscopy (SEM), atomic force microscopy (AFM) and contact angle (CA). Bone marrow mesenchymal cells (BMMCs) were seeded on four groups of titanium samples. Scanning electron microscopy (SEM) was employed to observe cell morphology. Cell proliferation was determined by MTT assay. The expression of focal adhesion proteins (F-actin; vinculin; osteocalcin, OCN; osteopontin, OPN) were observed under a confocal laser scanning microscope (CLSM). The mRNA expression levels of osteogenic factors (runt-related transcription factor 2, RUNX2; osteocalcin, OCN; osteopontin, OPN; collagen I, COL I) were assessed by qRT-PCR. **Results** The micro/nano- TiO_2 group featured a hydrophilic surface (CA = 9° ± 2.1°). The results of the MTT assay indicated that the relative cell proliferation rates for the nano- TiO_2 and micro/nano-TiO_2 samples were significantly increased compared with those for the untreated-Ti and micro-Ti samples ($P < 0.001$) after 5-9 days. The ALP results indicated that the micro/nano-TiO_2 sample gained the highest value at 14 days. After 72 h of incubation, the expression of osteocalcin (OCN) and osteopontin (OPN) on micro/nano-TiO_2 was the strongest. After 24 h incubation, the expression of F-actin on micro/nano-TiO_2 was the strongest. In comparison with untreated-Ti and micro-Ti samples, the mRNA expression levels of all the osteogenic factors (runt-related transcription factor 2, RUNX2; osteocalcin, OCN; osteopontin, OPN; Collagen I, COL I) were markedly increased on the nano-TiO_2 and micro/nano-TiO_2 samples, the mRNA expression levels of collagen I (COL I) were significantly different between the nano-TiO_2 and micro/nano-TiO_2 samples versus the untreated-Ti and micro-Ti samples ($P < 0.001$). **Conclusion** The novel biomimetic micro/nano hierarchical interface has a positive effect on cell attachment, viability and osteogenic differentiation of bone marrow mesenchymal cells.

【Key words】 micro/nano structure; TiO_2 nano-tubes; bionic; surface treatment; implants; bone marrow mesenchymal cells; cell adhesion; cell proliferation; osteogenic differentiation; spark plasma sintering; electrochemical anodization

J Prev Treat Stomatol Dis, 2021, 29(4): 226-233.

【Competing interests】 The authors declare no competing interests.

This study was supported by the grants from National Natural Science Foundation of China (No. 81901026)

骨内植入体在整形外科和牙科应用十分广泛[1-2]。低弹性模量的纯钛或钛合金是目前植入体的首选材料[3]。但钛及钛合金属于生物惰性材料，直接植入常无法获得良好快速的骨结合，制约了其更为广泛的应用。骨结合是骨内植入体植入成功的标志[4]，细胞在种植体表面黏附、增殖是种植体与周围组织作用的关键环节，通过影响细胞黏附、增殖、分化等细胞反应最终影响植入体骨结合性能[5-7]。如何通过种植体表面改性促进成骨细胞早期黏附，缩短植入体骨结合时间，增强骨结合强度，仍然是口腔种植体领域研究热点[8-10]。研究证实，通过电化学阳极氧化形成的纳米级表面形貌可以促进成骨细胞在植入体表面的早期附着[11]。同时，骨具有微纳米级共存的梯度结构[12]，从仿生角度，具有微纳米级共存的梯度仿生表面结构更利于植入体-周围骨组织营养运输和骨引导生长[13]。目前，钛材如何在三维空间中影响细胞-植入体的相互作用尚未达到共识。本研究制备一种新型微纳米共存的梯度仿生表面结构，即在微米骨小梁样结构上制备TiO_2纳米管结构，并研究其对体外大鼠骨髓间充质细胞（bone marrow mesenchymal cells，BMMCs）增殖、黏附及成骨向分化潜能的影响。

1　材料和方法

1.1　主要材料、试剂及仪器

纯钛材料（中国科学院金属研究所）；SPS-1050放电等离子烧结系统（Thermal Technology LLC，SantaRosa，CA，美国）；PGSTAT302N电化学工作站（Metrohm，中国）；4周大雄性SD大鼠（SYXK（川）2018-185）由四川大学动物实验中心提供；10%水合氯醛（四川大学华西妇产儿童医院）；胰蛋白酶、

胎牛血清、α-MEM培养基(Gibco,美国);MTT(Sigma-Aldrich,美国);碱性磷酸酶(alkaline phosphatase,ALP)检测试剂盒(Beyotime,中国);DAPI染色液(碧云天生物科技有限公司);DyLight 549标记的山羊抗兔二抗IgG、DyLight488标记的山羊抗鼠二抗IgG、兔抗鼠骨钙素(osteocalcin,OCN)抗体、鼠抗鼠骨桥蛋白(osteopontin,OPN)抗体、Alex Fluor647标记的Anti-Vinculin抗体、FITC-phalloidin(Millipore,美国);引物(Invitrogen,美国)、SYBR定量PCR试剂盒(Takara,日本);扫描电子显微镜(Inspect F,FEI,荷兰);原子力显微镜(Nanoscope Multi Mode & Expolre SPM, Vecco Instrument, 美国);倒置荧光显微镜(Olympus,日本);TL101接触角分析仪(TL101,Biolin scientific,瑞典),cDNA试剂盒(Takara,日本)。

1.2　材料制备及表征观察

1.2.1　材料制备　将纯钛试样预处理,依次用丙酮、去离子水超声清洗10 min,高温蒸汽灭菌后备用,命名为纯钛组。一组纯钛试件表面行放电等离子烧结处理,制备微米骨小梁样形貌,命名为微米骨小梁组;一组纯钛试件表面行阳极氧化处理,制备TiO_2纳米管形貌,命名为TiO_2纳米管组;一组纯钛表面首先通过放电等离子烧结法制备微米骨小梁样形貌,再通过阳极氧化法在微米骨小梁形貌上制备TiO_2纳米管结构,形成新型微纳米共存梯度仿生表面结构,命名为微纳米复合钛组。

1.2.2　表征观察　①表面形貌:扫描电子显微镜观察4组材料表面形貌,通过原子力显微镜进一步观察纯钛组和TiO_2纳米管组表面形貌,使用Nanoscope Multi Mode图形分析软件对样品表面的表面平均粗糙度均方根、表面积差值(三维表面积比二维表面积的比值增加的百分比)、垂直距离等表面粗糙度指标进行定量分析。

②表面能:利用静态水接触角实验检测不同植入材料表面能,每个样本表面随机选取5个点进行测量。

1.3　体外实验

1.3.1　大鼠骨髓间充质细胞分离和培养　取4周大雄性SD大鼠,10%水合氯醛腹腔注射麻醉后颈椎脱臼处死,浸泡于75%酒精。迅速分离胫骨和腓骨周围的皮肤、肌肉等结缔组织,将股骨和胫骨置于1%双抗溶液中。在无菌条件下,剪去股骨及胫骨的骨垢端,用无菌注射器吸取培养基冲洗骨髓腔获得细胞悬液,1 000 r/min离心5 min后用含10%胎牛血清的α-MEM培养基重悬,记为P0。37 ℃、体积分数为5%CO_2、饱和湿度的细胞培养箱孵育。48 h后首次换液,更换新鲜培养基,隔日换液,待细胞生长至80%~90%融合时按1∶3传代培养。在细胞超净台中,将第2~4代BMMCs以5×10^4/mL细胞密度接种于4组植入材料表面,置于37 ℃、5%CO_2、饱和湿度的培养箱中培养。在不同时间点进行如下检测。

1.3.2　细胞黏附情况　细胞接种2 h后,PBS清洗2次,2.5%戊二醛固定30 min,依次用20%、40%、60%、80%、90%酒精以及无水乙醇梯度脱水,每个梯度脱水10 min。将样本轻轻粘在导电胶上,临界点干燥、真空喷镀,行扫描电镜观察。

1.3.3　细胞增殖能力(MTT法)　细胞接种于4组材料表面1、3、5、7、9 d后,PBS清洗,每孔加入10 mg/mL的MTT 10 μL,37 ℃培养箱中孵化4 h,弃掉上清液,每孔再加入二甲亚砜150 μL,室温下孵育15 min充分震荡溶解沉淀,使用酶联免疫检测仪检测OD_{590} nm。每组样本在每个时间点选4个平行样进行检测,以纯钛组接种细胞第1天检测的结果为参照,计算各组细胞相对增殖率。

1.3.4　碱性磷酸酶检测　钛材样品接种细胞24 h后,将培养基更换为成骨诱导液(含体积分数10%的胎牛血清,地塞米松100 nmol/L、抗坏血酸50 mg/L、β-甘油磷酸钠10 mmol/l的α-MEM培养液)。每48 h换液1次。培养7、10、14 d后,PBS清洗3次,每孔加入0.2%Triton-X-100裂解液400 μL,放置4 ℃过夜。次日细胞裂解液50 μL和50 μL对硝基苯磷酸盐(p-nitrophenyl phosphate, PNPP)孵育30 min后每孔加入100 μL反应终止液终止反应,使用酶联免疫检测仪在OD_{405} nm。同时按照BCA蛋白定量试剂盒说明书操作测定总蛋白浓度。每组样本在每个时间点选4个平行样进行检测。

1.3.5　免疫荧光检测细胞黏着斑蛋白、成骨分化相关蛋白表达　接种24 h后,PBS清洗3次,4%多聚甲醛固定30 min,0.2% Triton X-100通透15 min,避光、4 ℃条件下Alex Fluor647标记的Anti-Vinculin抗体、FITC-phalloidin对各组表面上附着的细胞进行染色并过夜。

接种72 h后,PBS清洗3次,4%多聚甲醛固定30 min,0.2% Triton X-100通透细胞膜15 min,观察OCN、OPN表达。一抗孵育:吸水纸吸掉封闭液,每张爬片上滴加足够量稀释好的一抗(OCN 1∶200;OPN 1∶200)并放入湿盒,4 ℃过夜;二抗孵育:

取出湿盒，37 ℃下复温45 min，PBS清洗爬片3次，吸水纸吸掉残留的PBS，滴加稀释好的DyLight 549标记的二抗Ig G（1∶500）、DyLight488标记的二抗IgG（1∶500）。

最后均用DAPI避光染色5 min。激光共聚焦显微镜（confocal laser scanning microscopy，CLSM）下观察。

1.3.6　qRT-PCR检测成骨标志基因表达　细胞接种7 d后，用Trizol试剂提取总RNA，使用1步法cDNA试剂盒逆转录成cDNA，再行qRT-PCR检测。引物序列如表1所示。PCR反应条件：95 ℃预变性30 s，95 ℃变性5 s，60 ℃退火30 s，运行40个循环，目的基因表达均依据管家基因GAPDH表达水平进行标准化处理后进行比较，根据$2^{-\Delta\Delta Ct}$法对成骨标志基因：RUNX2、OCN、OPN和Ⅰ型胶原（collagen type Ⅰ，COL Ⅰ）进行基因相对表达倍数转化。

1.4　统计学分析

采用IBM SPSS 19.0软件进行数据分析，结果均以$\bar{x} \pm s$来表示，采用单因素方差分析及q检验进行组间比较，$P < 0.05$为差异有统计学意义。

表1　PCR引物序列

Table 1　Specific prime sequences of PCR

Gene	Forward primer 5′-3′	Reverse primer 5′-3′
COL Ⅰ	GCTGGCAAGAATGGCGAC	AGCCACGATGACCCTTTATG
OCN	GGAGGGCAGTAAGGTGGTGA	ACGGTGGTGCCATAGATGC
OPN	AACAGTATCCCGATGCCACA	TGGCTGGTCTTCCCGTTG
RUNX2	CAGGCGTATTTCAGATGATGACA	TAAGTGAAGGTGGCTGGATAGTG
Actin	CCCATCTATGAGGGTTACGC	TTTAATGTCACGCACGATTTC

COL Ⅰ: collagen type Ⅰ; OCN: osteocalcin; OPN: osteopontin; RUNX2: runt-related transcription factor 2

2　结　果

2.1　样品表征

2.1.1　材料表面形貌特点分析　扫描电子显微镜下纯钛组表面仅见机械打磨的痕迹（图1a）；微米骨小梁组表面形成微米骨小梁样表面形貌，有些微米管之间互相交通（管径30～100 μm），类似骨小梁结构（图1b）；TiO_2纳米管组表面形成均一排列的TiO_2纳米管样结构（图1c、图1d）；微纳米复合钛组表面形成微米骨小梁结构上有均一排列TiO_2纳米管的新型梯度仿生表面结构。

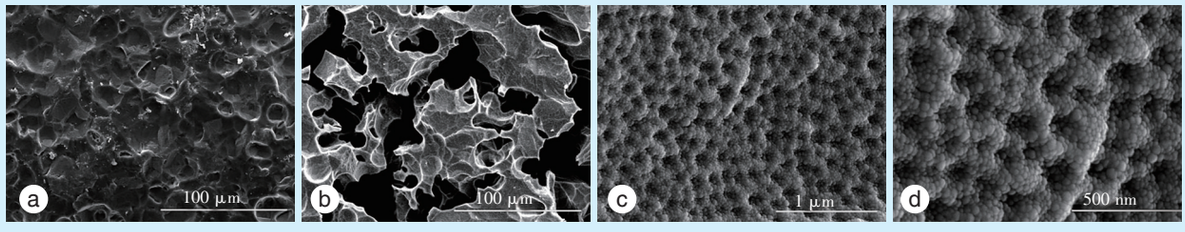

a: untreated-Ti (× 1 000); b: microporous trabecular bone-like architecture (×1 000). It resembled a trabecular bone; c: TiO_2 nano-pores arranged uniformly (× 80 000); d: TiO_2 nano-pores arranged uniformly (× 160 000); SEM: scanning electronmicroscopy

Figure 1　SEM images of the surface of titanium samples

图1　材料表面形貌扫描电镜观察

原子力显微镜下可见纯钛组表面光滑，没有明显的孔洞或任何规则的形状；TiO_2纳米管组纳米孔近似圆形，直径从十几纳米至上百纳米不等，纳米孔深度从十几至几十纳米不等（图2）。AFM粗糙度的定量分析结果见表2，TiO_2纳米管组表面比纯钛组粗糙（$P < 0.001$），TiO_2纳米管组表面粗糙度、轮廓最大高度偏差、表面积差值分别约为纯钛组的2.9倍、2.2倍、1.9倍。

2.1.2　材料表面的表面能检测　4组材料表面的表面能检测结果显示（图3）：静态水接触角分别为35° ± 2.3°（纯钛组）、18° ± 1.6°（微米骨小梁组）、14° ± 1.6°（TiO_2纳米管组）和9° ± 2.1°（微纳米复合钛组）。微纳米复合钛组的静态水接触角最小（$P < 0.001$），说明其表面亲水性最好。

2.2　体外材料表面细胞行为

2.2.1　细胞黏附情况　4组材料表面接种4 h后细胞黏附情况显示，纯钛组细胞多呈梭形，部分可见伪足和触角（图4a）。微米骨小梁组细胞呈扁平多角形，可明显见伪足和触角（图4b）。TiO_2纳米管组细胞扁平多角形，紧密附着在材料表面（图4c）。微纳米复合钛组细胞伸展更加充分，细胞与细胞间相互交织连接，大多成片，可见大量伪足和触角（图4d）。

2.2.2　细胞增殖能力（MTT）　BMMCs接种4组材

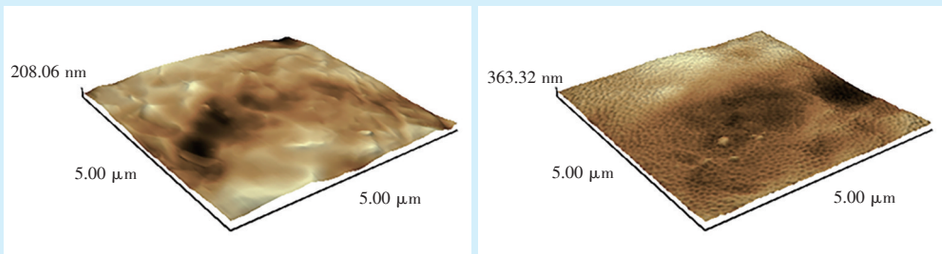

a: untreated-Ti group, which showed a relatively rough surface; b: nano-TiO_2 group; nano-pores (diameter: 50-120 nm) were observed on its surface; AFM: atomic force microscopy

Figure 2　AFM images of samples in the untreated-Ti group and nano-TiO_2 group

图2　纯钛组和TiO_2纳米管组表面AFM扫描图

表2　纯钛组和TiO_2纳米管组表面参数比较

Table 2　Surface parameters of samples in the untreated-Ti group and nano-TiO_2 group

Group	Surface roughness (nm)	Vertical range (nm)	Surface difference (%)
Untreated-Ti	15.89 ± 2.5	156.53 ± 30.31	7.35 ± 2.18
Nano-TiO_2	46.30 ± 2.18[1)]	340 ± 33.56[1)]	13.78 ± 2.58[1)]

1): the untreated-Ti group *vs* the nano-TiO_2 group, $P < 0.05$

料表面增殖活性MTT检测结果如图5所示。接种后1～9 d细胞增殖活性呈递增趋势，但1 d和3 d差异无统计学意义（$P = 0.278$），结果表明，1～4 d，微纳米复合钛组和TiO_2纳米管组细胞增殖活性高于纯钛组和微米骨小梁组，但差异没有统计学意义。5～9 d，微纳米复合钛组和TiO_2纳米管组的细胞增殖活性显著高于纯钛组和微米骨小梁组（$P < 0.001$）。

2.2.3　ALP活性　BMMCs接种4组材料表面7、10、

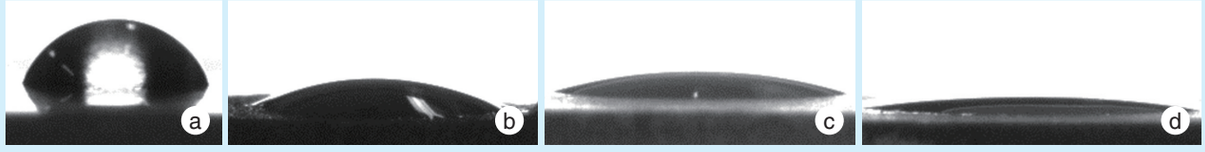

a: untreated-Ti group, 35° ± 2.3°; b: micro-Ti group, 18° ± 1.6°; c: nano-TiO_2 group, 14° ± 1.6°; d: micro/nano-TiO_2 group, 9° ± 2.1°

Figure 3　The static contact angles on the samples in the four groups

图3　4组材料表面静态接触角

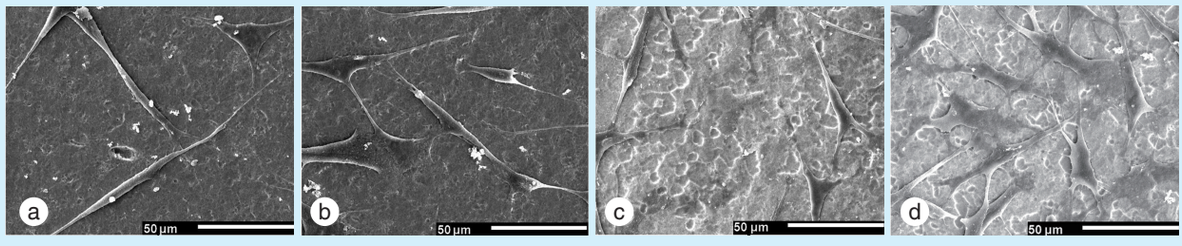

a: untreated-Ti group, most of the cells were fusiform, some of which can be seen with pseudopodia and antennas; b: micro-Ti group, the cells were flat and polygonal, with pseudopodia and antennas clearly visible; c: nano-TiO_2 group, the cells were flat and polygonal, closely attached to the surface of the titanium samples; d: micro/nano-TiO_2 group, cells were connected with each other and grew together flakily, with large numbers of pseudopodia and antennas; SEM: scanning electronmicroscopy

Figure 4　SEM images of BMMCs 4 h after culture on the surfaces of samples in the four groups

图4　骨髓间充质细胞接种于4组钛材表面4 h后的扫描电镜图

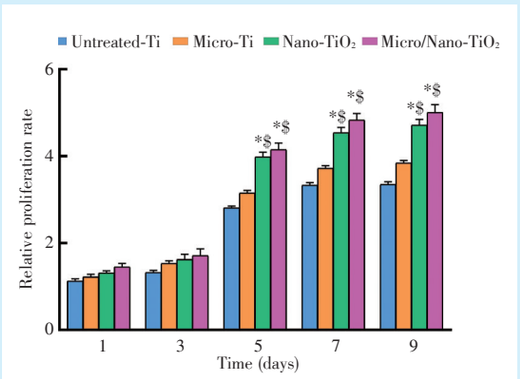

*: *vs.* untreated-Ti group, $P < 0.05$; $: *vs.* micro-Ti group, $P < 0.05$. The relative cell proliferation rates of samples in the four groups increased between days 1-9, and the relative cell proliferation rates of samples in the nano-TiO_2 group and the micro/nano-TiO_2 group significantly increased compared with those in the untreated-Ti group and the micro-Ti group($P < 0.001$) between days 5-9

Figure 5　The cell proliferation rate of BMMCs cultured on the samples in the four groups

图5　BMMCs接种于4组材料表面后的细胞相对增殖率

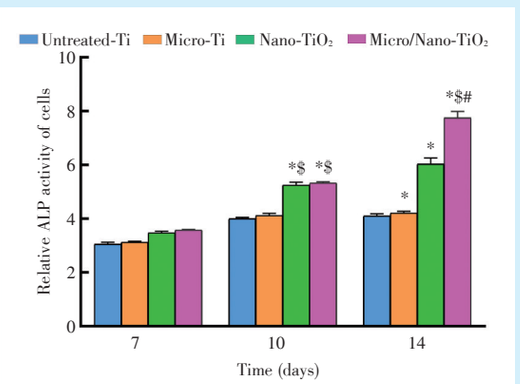

*: *vs.* untreated-Ti group, $P < 0.05$; $: *vs.* micro-Ti group, $P < 0.05$; #: *vs.* nano-TiO_2 group, $P < 0.05$. The relative cell proliferation rates of samples in the four groups increased between days 7-14, and the samples in the micro/nano-TiO_2 group gained the highest value on the 14th day

Figure 6　ALP activity of BMMCs cultured on the samples in the four groups

图6　BMMCs接种于4组材料表面后的细胞ALP活性

14 d ALP活性检测结果如图6。细胞在4组材料表面ALP活性在7～14 d呈递增趋势。10 d和14 d时，TiO_2纳米管组和微纳米复合钛组表面细胞ALP活性明显高于纯钛组（$P < 0.001$）。14 d时，微纳米复合钛组表面ALP活性最高，说明微纳米复合钛表面促进骨髓间充质细胞成骨向分化。

2.2.4　细胞黏附、成骨分化相关蛋白表达　培养24 h后，纯钛组黏着斑蛋白染色较微米骨小梁组、TiO_2纳米管组和微纳米复合钛组浅，微米管组、TiO_2纳米管组和微纳米复合钛组之间无明显差异；TiO_2纳米管组和微米骨小梁组中肌动蛋白染色深于纯钛组，微纳米复合钛组肌动蛋白染色最深（图7a）。

培养72 h后，纯钛组表达OCN和OPN最弱，微纳米复合钛组表达OCN，OPN比微米骨小梁组和TiO_2纳米管组强（图7b）。

2.2.5　qRT-PCR检测成骨标志基因表达　TiO_2纳米管组和微纳米复合钛组表面细胞所有成骨转录因子的基因表达水平高于纯钛组和微米骨小梁组，其中COL I基因表达水平有显著性差异（$P < 0.001$）。结果表明TiO_2纳米管组和微纳米复合钛组促进BMMCs早期成骨转化。纯钛组的OPN和OCN基因表达水平最低，与细胞免疫荧光染色结果一致（图8）。

3　讨　论

骨结合是骨内植入体植入成功的标志，良好的骨结合说明人体骨组织与植入体表面形成直接稳定连接，有利于抗压和负重[14]。植入体骨结合效果受其表面性质（如粗糙程度、表面形貌等）的影响，可以通过表面改性增强其骨结合性能，如放电等离子烧结、酸蚀、阳极氧化[15-17]。骨具有微纳米级共存的梯度结构，从仿生角度，具有微纳米级共存的梯度仿生表面结构更利于植入体-周围骨组织营养运输和骨引导生长。研究证实微纳米复合钛表面形貌骨结合性能优于微米管和TiO_2纳米管表面形貌[18]。本研究制备出一种新型微纳米共存梯度仿生表面结构，首先通过放电等离子烧结法在纯钛表面制备微米骨小梁样结构，再通过阳极氧化法在微米骨小梁样结构上制备TiO_2纳米管结构，形成新型微纳米共存梯度仿生表面结构，将BMMCs接种于新型微纳米共存梯度仿生表面结构表面，探究其对大鼠骨髓间充质细胞生物学活性的影响。

MTT细胞增殖结果显示，1～9 d，微纳米复合钛组和TiO_2纳米管组细胞增殖活性高于纯钛组和微米骨小梁组；5～9 d，微纳米复合钛组和TiO_2纳米管组的增殖活性显著高于纯钛组和微米骨小梁

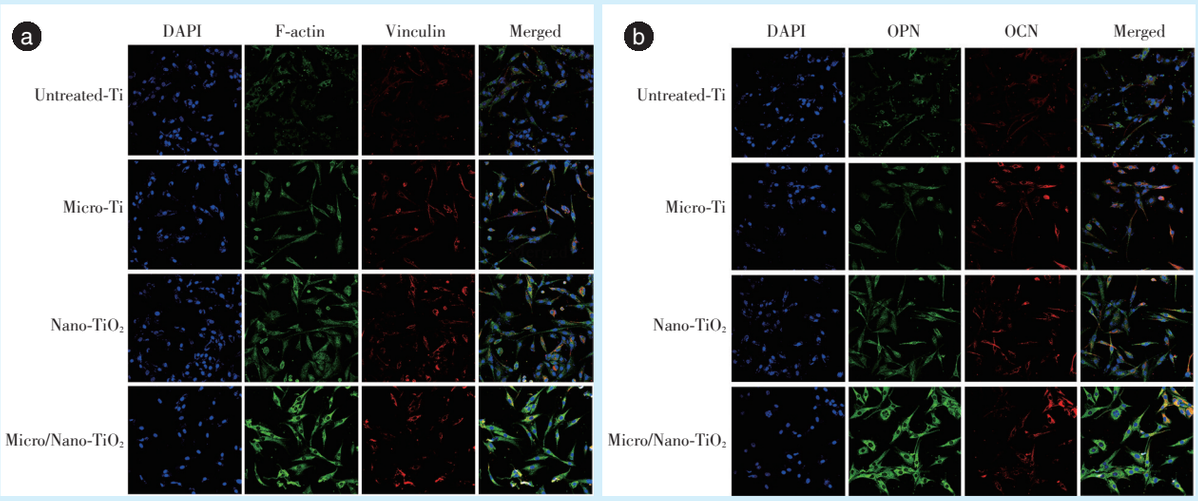

a: the expression of F-actin and vinculin after 24 h incubation. The expression of F-actin in the micro/nano-TiO_2 group was the strongest. b: the expression of OCN and OPN after 72 h incubation. The expression of OCN and OPN in the micro/nano-TiO_2 group was the strongest. Blue: cell nucleus; green: either F-actin or OPN; red: either vinculinor or OCN; OCN: osteocalcin; OPN: osteopontin

Figure 7　Immunofluorescence staining images of BMMCs cultured on the samples in the four groups　(× 400)

图7　BMMCs接种于4组材料表面的细胞免疫荧光染色图　(× 400)

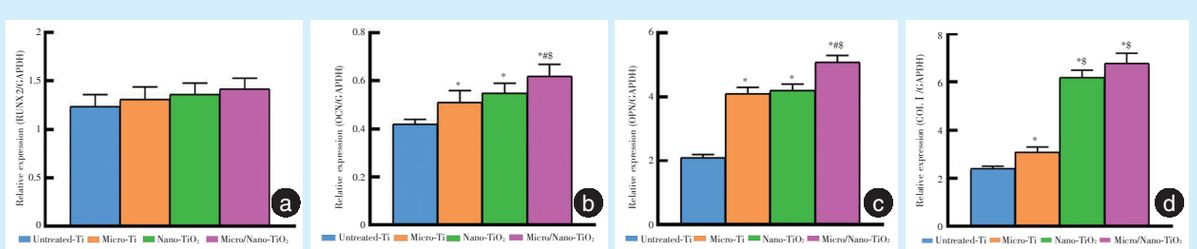

a: RUNX2; b: OCN; c: OPN; d: COL Ⅰ (collagen I). *$P < 0.05$ *vs.* untreated-Ti group, #: $P < 0.05$ *vs.* micro-Ti group, $: $P < 0.05$ *vs.* Nano-TiO_2 group. Compared with the untreated-Ti group and the micro-Ti group, the mRNA expression levels of all the osteogenic factors in the nano-TiO_2 and micro/nano-TiO_2 groups markedly increased; compared with the untreated-Ti group and micro-Ti group, the mRNA expression levels of COL I in the nano-TiO_2 and micro/nano-TiO_2 groups significantly increased ($P < 0.001$)

Figure 8　mRNA expression levels of various osteogenic transcription factors in the four groups

图8　4组成骨转录因子mRNA表达

组；提示联合应用放电等离子烧结和阳极氧化处理的钛表面表面接种的BMMCs增殖活性更好。ALP是成骨分化的早期标志，可水解磷酸离子，形成羟基磷灰石晶体并促进矿化[19]。成骨诱导10 d和14 d，TiO_2纳米管组和微纳米复合钛组表面细胞ALP活性明显高于纯钛组（$P < 0.001$），证实联合应用放电等离子烧结和阳极氧化处理的钛表面可促进BMMCs成骨分化。

CLSM结果示微纳米复合钛组和TiO_2纳米管组OCN、OPN染色深于纯钛组和微米管组。qRT-PCR结果示TiO_2纳米管组和微纳米复合钛组表面细胞的RUNX2、OCN、OPN和COL I基因表达水平强于纯钛组和微米骨小梁组，I型胶原表达水平有显著性差异（$P < 0.001$）。结果表明微纳米复合钛组可促进细胞黏附、增殖以及成骨向分化。

综上所述，联合应用放电等离子体烧结和阳极氧化法在纯钛植入体表面制备的新型微纳米共存的梯度仿生表面结构可促进骨髓间充质细胞的黏附、增殖及成骨向分化。下一步将进行动物体内实验，进一步证实改性钛表面的成骨活性。

【Author contributions】 Wang M peformed the experiments, analyzed the data, and wrote the article. Jiang N revised the article. Zhu ZS designed the study. All authors read and approved the final manuscript as submitted.

参考文献

[1] Jaggessar A, Shahali H, Mathew A, et al. Bio-mimicking nano and micro-structured surface fabrication for antibacterial properties in medical implants[J]. J Nanobiotechnology, 2017, 15(1): 64. doi: 10.1186/s12951-017-0306-1.

[2] Li T, Gulati K, Wang N, et al. Understanding and augmenting the stability of therapeutic nanotubes on anodized titanium implants [J]. Mater Sci Eng C Mater Biol Appl, 2018, 88: 182-195. doi: 10.1016/j.msec.2018.03.007.

[3] Ahn TK, Lee DH, Kim TS, et al. Modification of titanium implant and titanium dioxide for bone tissue engineering[J]. Adv Exp Med Biol, 2018, 1077: 355-368. doi: 10.1007/978-981-13-0947-219.

[4] Zhao C, Wang X, Gao L, et al. The role of the micro-pattern and nano-topography of hydroxyapatite bioceramics on stimulating osteogenic differentiation of mesenchymal stem cells[J]. Acta Biomater, 2018, 73: 509-521. doi: 10.1016/j.actbio.2018.04.030.

[5] Zhukova Y, Hiepen C, Knaus P, et al. The Role of titanium surface nanostructuring on preosteoblast morphology, adhesion, and migration[J]. Adv Healthc Mater, 2017, 6(15): 201601244. doi: 10.1002/adhm.201601244.

[6] Llopis-Grimalt MA, Amengual-Tugores AM, Monjo M, et al. Oriented cell alignment induced by a nanostructured titanium surface enhances expression of cell differentiation markers[J]. Nanomaterials, 2019, 9(12): 1661. doi: 10.3390/nano9121661.

[7] Duvvuru MK, Han W, Chowdhury PR, et al. Bone marrow stromal cells interaction with titanium:effects of composition and surface modification[J]. PLoS One, 2019, 14(5): e0216087. doi: 10.1371/journal.pone.0216087.

[8] Yuan Z, Liu P, Hao Y, et al. Construction of Ag-incorporated coating on Ti substrates for inhibited bacterial growth and enhanced osteoblast response[J]. Colloids Surf B Biointerfaces, 2018, 171: 597-605. doi: 10.1016/j.colsurfb.2018.07.064.

[9] Li W, Yang Y, Zhang H, et al. Improvements on biological and antimicrobial properties of titanium modified by AgNPs-loaded chitosan-heparin polyelectrolyte multilayers[J]. J Mater Sci Mater Med, 2019, 30(5): 52. doi: 10.1007/s10856-019-6250-x.

[10] Zhong X, Song Y, Yang P, et al. Titanium surface priming with phase-transited lysozyme to establish a silver nanoparticle-loaded chitosan/hyaluronic acid antibacterial multilayer via layer-by-layer self-assembly[J]. PLoS One, 2016, 11(1): e0146957. doi: 10.1371/journal.pone.0146957.

[11] Jang I, Choi DS, Lee JK, et al. Effect of drug-loaded TiO_2 nanotube arrays on osseointegration in an orthodontic miniscrew: an *in-vivo* pilot study[J]. Biomed Microdevices, 2017, 19(4): 94. doi: 10.1007/s10544-017-0237-5.

[12] Zhao H, Chang CC, Liu Y, et al. Reproducibility and radiation effect of high-resolution *in vivo* micro computed tomography imaging of the mouse lumbar vertebra and long bone[J]. Ann Biomed Eng, 2020, 48(1): 157-168. doi: 10.1007/s10439-019-02323-z.

[13] 许嘉允, 邓飞龙, 庄秀妹, 等. 纯钛微纳米复合形貌对成骨细胞生物学行为的影响[J]. 中华口腔医学研究杂志, 2015, 9(6): 461-469. doi: 10.3877/cma.j.issn.1674-1366.2015.06.005.
Xu JY, Deng FL, Zhuang XM, et al. The influence of different hybrid micro/nano hierarchical titanium topographies on osteoblast biological functions[J]. Chin J Stomatol, 2015, 9(6): 461-469. doi: 10.3877/cma.j.issn.1674-1366.2015.06.005.

[14] 罗翠芬, 彭国光, 冯远华, 等. 激素对种植体骨结合影响的研究进展[J]. 口腔疾病防治, 2017, 25(7): 473-476. doi: 10.12016/j.issn.2096-1456.2017.07.015.
Luo CF, Peng GG, Feng YH, et al. Influence of hormones on osseointegration in dental implant[J]. J Prev Treat Stomotol Dis, 2017, 25(7): 473-476. doi: 10.12016/j.issn.2096-1456.2017.07.015.

[15] Jang TS, Jung HD, Kim S, et al. Multiscale porous titanium surfaces *via* a two-step etching process for improved mechanical and biological performance[J]. Biomed Mater, 2017, 12(2): 025008. doi: 10.1088/1748-605X/aa5d74.

[16] Zahran R, Leal JIR, Valverde MAR, et al. Effect of hydrofluoric acid etching time on titanium topography, chemistry, wettability, and cell adhesion[J]. PLoS One, 2016, 11(11): e0165296. doi: 10.1371/journal.pone.0165296.

[17] Ma XJ, Li M, Meng F, et al. Efficient nano titanium electrode *via* a two-step electrochemical anodization with reconstructed nanotubes: electrochemical activity and stability[J]. Chemosphere, 2018, 202: 177-183. doi: 10.1016/j.chemosphere.2018.03.063.

[18] Xu D, Wan Y, Li Z, et al. Tailorable hierarchical structures of biomimetic hydroxyapatite micro/nano particles promoting endocytosis and osteogenic differentiation of stem cells[J]. Biomaterials, 2020, 8(12): 3286-3300. doi:10.1039/d0bm00443j.

[19] Pan X, Li Y, Abdullah AO, et al. Micro/nano-hierarchical structured TiO(2) coating on titanium by micro-arc oxidation enhances osteoblast adhesion and differentiation[J]. R Soc open Sci, 2019, 6 (4): 182031. doi: 10.1098/rsos.182031.

(编辑　张琳,曾曙光)